

# Studies on the corrosion behavior of yttrium-implanted zircaloy-4

JIAN XU\*, XINDE BAI, YUDIAN FAN

*Department of Materials Science and Engineering, Tsinghua University, Beijing 100084, People's Republic of China*

*E-mail: xujian1999@263.net*

WENLIANG LIU, HONGBIN BEI

*Beijing General Research Institute for Non-Ferrous Metals, Beijing 100088, People's Republic of China*

In order to study the effects of yttrium ion implantation on the aqueous corrosion behavior of zircaloy-4, specimens were implanted with yttrium ions using a MEVVA source at an energy of 40 keV, with a dose range from  $1 \times 10^{16}$  to  $1 \times 10^{17}$  ions/cm<sup>2</sup> at about 150°C. Transmission electron microscopy (TEM) was used to obtain the structural character of the yttrium-implanted zircaloy-4. The valence of the yttrium ions in the surface layer was analyzed by X-ray photoemission spectroscopy (XPS). Three-sweep potentiodynamic polarization measurement was employed to evaluate the aqueous corrosion behavior of zircaloy-4 in a 1 N H<sub>2</sub>SO<sub>4</sub> solution. It was found that a significant improvement was achieved in the aqueous corrosion resistance of zircaloy-4 compared with that of the as-received zircaloy-4. The mechanism of the corrosion resistance improvement of the yttrium-implanted zircaloy-4 is probably due to the addition of the yttrium oxide dispersoid into the zirconium matrix. © 2000 Kluwer Academic Publishers

## 1. Introduction

Zirconium alloys are often specified for engineering use in the nuclear industry because of their low thermal neutron capture cross section, good corrosion resistance, and adequate mechanical properties. However, with the concept of high burn-up developing, the demand upon zirconium alloys becomes higher. It is known that certain modification methods, such as ion beam surface processing (IBP), can significantly improve the corrosion resistance [1, 2]. Ion implantation, a kind of IBP, offers the possibility to introduce a controlled concentration of an element to a thin surface layer rapidly. It was first shown, by Ashworth *et al.*, that chromium implantation improved the corrosion resistance of iron [3]. Then, there is a growing interest in the application of ion implantation, as a valuable process for surface modification of materials. Many studies including palladium implanted into titanium [4], phosphorous implanted into iron [5], and molybdenum and tantalum co-implanted into titanium [6] have proved that ion implantation can successfully improve the corrosion resistance without affecting the physical and mechanical stability of the bulk material.

Recently, the studies of yttrium ion implantation have been devoted to investigation of the high temperature oxidation behavior of metals [7, 8]. Little attention has been paid to improving the aqueous corrosion resistance.

In this paper, the aqueous corrosion behavior of zircaloy-4 implanted by yttrium ions was studied. The structure of implanted layer was investigated by TEM, and the valence of the yttrium ions was determined by XPS. The mechanism of the aqueous corrosion resistance improvement of the yttrium-implanted zircaloy-4 is discussed.

## 2. Experimental details

The samples were machined to 10 mm × 10 mm from a zircaloy-4 sheet fully annealed after cold rolling, the thickness of which was 1.5 mm. The composition of zircaloy-4 is Sn: 1.4 wt.%, Fe: 0.23 wt.%, Cr: 0.1 wt.%, Ni:  $60 \times 10^{-6}$  wt.%, balanced with zirconium. The samples were mechanically polished with 200–800 grade emery paper, then degreased in acetone and ethanol, chemically polished in the solution of 10 vol.% HF, 30 vol.% HNO<sub>3</sub>, 60 vol.% H<sub>2</sub>O, rinsed in natural water more than three times and finally rinsed in deionized water. The samples used for transmission electron microscope (TEM) examination were prepared by sputtering deposition of a 50–60 nm thin zircaloy-4 film on single crystal NaCl.

Zircaloy-4 samples were loaded onto a steel-made sample holder in the target chamber of the MEEVA implanter at a vacuum level of  $1 \times 10^{-4}$  Pa. The implanted area has a diameter of 12 cm. The yttrium implantation was carried out at an extracted voltage of 40 kV, and the

\* Author to whom all correspondence should be addressed.

beam current density was  $10 \mu\text{A}/\text{cm}^2$ . During implantation, no special cooling was used for the samples and the maximum temperature of the samples was  $150^\circ\text{C}$ . As the implantation system has no analysis magnet, the extracted yttrium ions were measured to consist of 5%  $\text{Y}^+$ , 60%  $\text{Y}^{2+}$ , and 33%  $\text{Y}^{3+}$ . Therefore, the implantation energies were 40, 80, and 120 keV for the  $\text{Y}^+$ ,  $\text{Y}^{2+}$ , and  $\text{Y}^{3+}$ , respectively. The implanted ions were at normal dose range from  $1 \times 10^{16}$  to  $1 \times 10^{17}$  ions/ $\text{cm}^2$ .

The structural character of the implanted layer was studied using a HITACHI H-800 transmission electron microscope (TEM). The valence of the yttrium ions in the surface layer was analyzed by X-ray photoemission spectroscopy (XPS).

In order to investigate the aqueous corrosion behavior of the yttrium-implanted zircaloy-4, the three-sweep potentiodynamic polarization measurements were carried out. Potentiodynamic tests were performed in a 1 N  $\text{H}_2\text{SO}_4$  solution using an EG&G PARC MODEL 351 potentiostat at room temperature ( $25^\circ\text{C}$ ). The working area was  $1 \text{ cm}^2$  and the scan rate was  $1 \text{ mV}/\text{s}$ . All electrochemical potential measurements were taken with respect to a saturated calomel electrode (SCE). The potentiodynamic polarization measurements were carried out as follow: an anodic scan was conducted starting in a cathodic region of approximately  $-0.3 \text{ V}$  with respect to the SCE and scanned into the anodic region of approximately  $+2.0 \text{ V}$  with respect to the SCE.

### 3. Results and discussions

#### 3.1. The structural character of the yttrium-implanted zircaloy-4

The morphology and structure of the implanted-zircaloy-4 samples were examined by TEM. Although the grain size of the sputtered film may be different with that of the 1.5 mm sheet, the structural transmission of the 1.5 mm sheet can be simulated by TEM studies of the sputtered film when the implanted dose is high enough [5]. Fig. 1a and b show the polycrys-

talline structure obtained for the unimplanted zircaloy-4. Fig. 2a and b show the polycrystalline structure of the zircaloy-4 sample implanted with  $1 \times 10^{17}$  ions/ $\text{cm}^2$  yttrium ions. Compared Fig. 1 with Fig. 2, it is clear that when the dose increased up to  $1 \times 10^{17}$  ions/ $\text{cm}^2$ , the structure is still polycrystalline. That means the structure of the surface layer is not significantly changed by yttrium ion implantation.

In some previous researches, it has been reported that the improvement of the corrosion resistance by ion implantation can be attributed to the structural transformation from crystalline to amorphous [5, 7]. This phenomenon did not occur in our experiment. The difference is due to the temperature of the samples during implantation. In ref. [5] and [7], the samples were implanted at liquid nitrogen temperature. However, the samples in our experiment were implanted at  $150^\circ\text{C}$ .

As we know, ion beam implantation always brings all kinds of defects, such as point defects and dislocation loops, to the surface of the materials. The existence of these defects will damage materials and change their structure. If the implantation is conducted at liquid nitrogen temperature, most defects can be preserved. Owing to the accumulation of the defects, the structure can transform from crystalline to amorphous. In our experiment, the large number of defects, which formed during the yttrium implantation recovered at  $150^\circ\text{C}$ . Thus, the structure is still polycrystalline. Therefore, the property improvement by the yttrium ion implantation is not mainly attributed to the structural change in the zircaloy-4 surface.

#### 3.2. The valence of the yttrium ions in the surface layer

The valence of the yttrium ions in the surface layer was analyzed by XPS. From the observation of the XPS spectra, the yttrium ion is probably incorporated in the film as oxide. Fig. 3a and b are the experimental XPS spectra of C1s, Y 3d<sub>5/2</sub>, respectively. In Fig. 3a, the

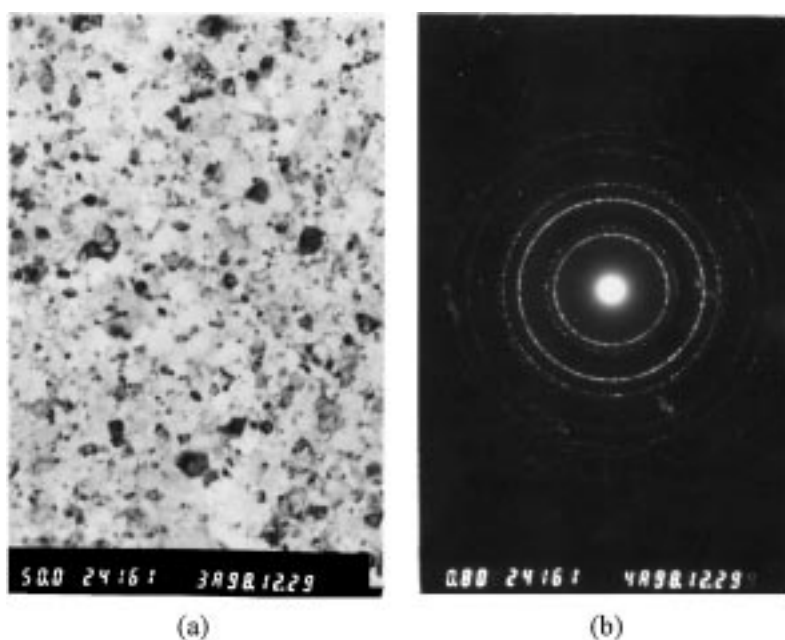


Figure 1 TEM of as-received zircaloy-4 (a) bright field image; (b) SAD pattern.

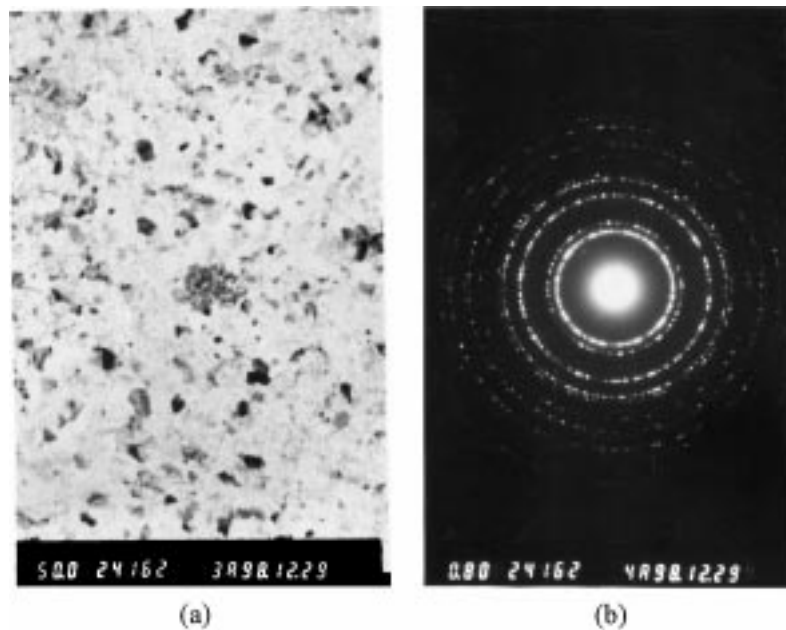


Figure 2 TEM of yttrium implanted zircaloy-4 at a dose of  $1 \times 10^{17}$  ions/cm<sup>2</sup> (a) bright field image; (b) SAD pattern.

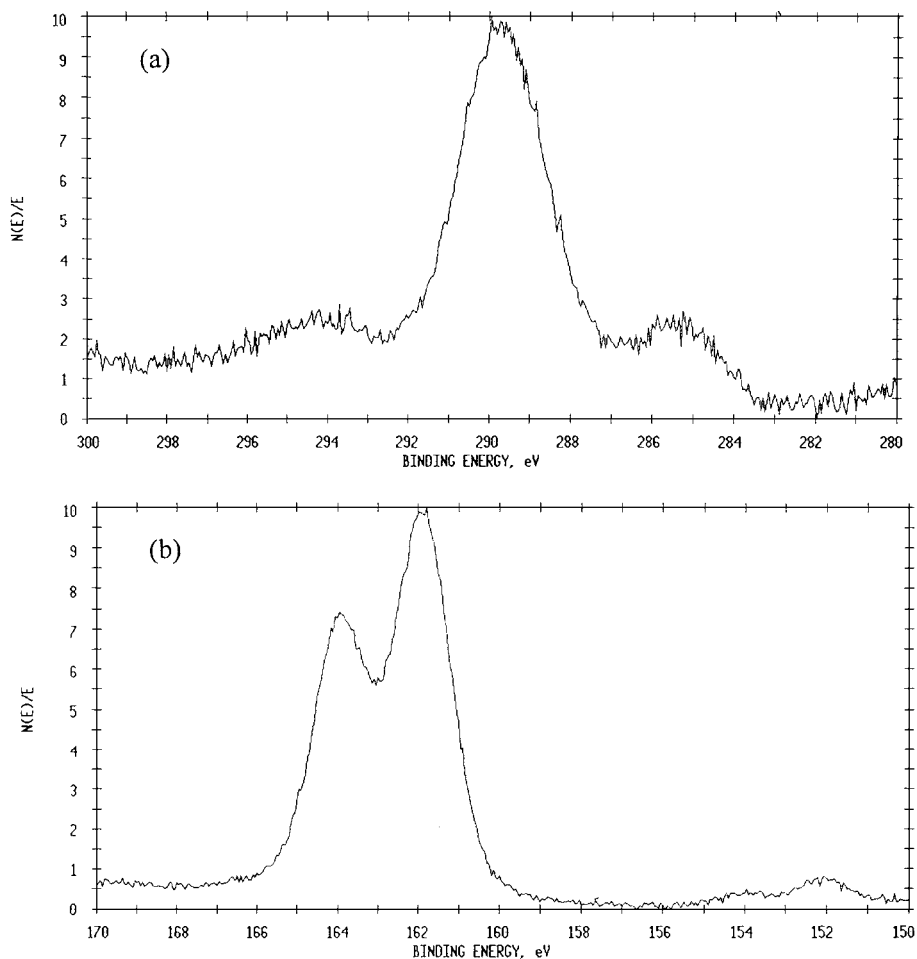


Figure 3 The XPS spectra of (a) C1s peak (b) Y 3d<sub>5/2</sub> peak in the implanted surface.

surface energy of the absorbed C on the surface of the specimen is 289.7 eV, which is 4.9 eV higher than the standard binding energy, 284.8 eV. The energy margin is due to the system error, and needs to be adjusted. The adjusted binding energy of the yttrium ions is 158.9 eV, which coincides well with the standard values of Y<sub>2</sub>O<sub>3</sub>. So, it can be said that the oxide of yttrium in the surface exists in the form of Y<sub>2</sub>O<sub>3</sub>.

### 3.3. The electrochemical properties of the yttrium-implanted zircaloy-4

The elements on the implanted surface were detected using auger electron spectroscopy (AES). It was found that there exists a great deal of oxygen in the surface layer of the yttrium-implanted zircaloy-4. In order to study the electrochemical performance of a freshly exposed and oxide-free surface, the three-sweep

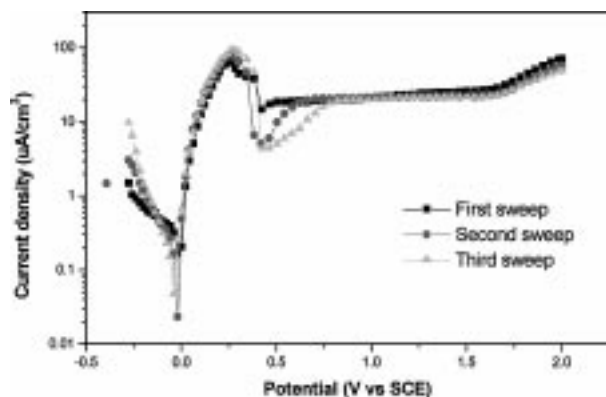


Figure 4 The three-sweep potentiodynamic polarization curves of the as-received zircaloy-4 in a 1 N H<sub>2</sub>SO<sub>4</sub> solution.

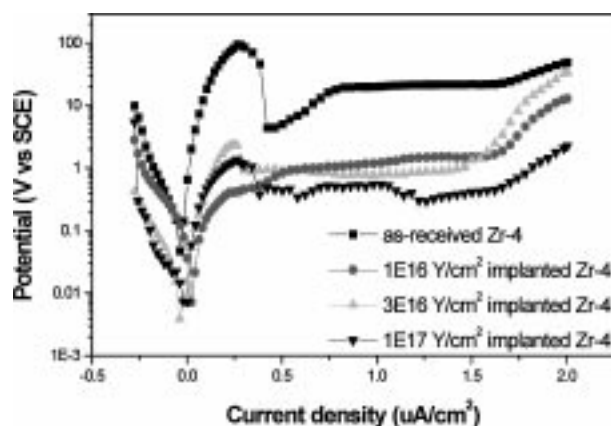


Figure 5 The third sweep potentiodynamic polarization curves of the as-received zircaloy-4 and the zircaloy-4 implanted with yttrium ions at a dose range from  $1 \times 10^{16}$  to  $1 \times 10^{17}$  ions/cm<sup>2</sup>.

potentiodynamic measurement was employed to eliminate the impact of thickened oxide film formed in air on the freshly implanted surface.

Fig. 4 summarizes the three-sweep potentiodynamic polarization curves of the as-received zircaloy-4 in a 1 N H<sub>2</sub>SO<sub>4</sub> solution. It can be seen that the potentiodynamic polarization curve of the freshly exposed oxide-free surface is represented by the third sweep. This result is corresponding to previous results [5, 9].

For clarity, the third sweep potentiodynamic polarization curves of the as-received zircaloy-4 and the zircaloy-4 implanted by yttrium ions at a dose range from  $1 \times 10^{16}$  to  $1 \times 10^{17}$  ions/cm<sup>2</sup> are summarized in Fig. 5. The dependence of the passive current density,  $i_p$ , on the implanted dose is given in Fig. 6.

Comparing the corrosion behavior of the yttrium-implanted zircaloy-4 to that of the as-received zircaloy-4 in Fig. 5 and Fig. 6, it is clear that the passive current density,  $i_p$  is decreased when the implanted dose increases. It indicates that the aqueous corrosion resistance of zircaloy-4 is significantly improved by yttrium ion implantation.

### 3.4. The mechanism of the improvement of the aqueous corrosion resistance by yttrium ion implantation

The formation of the passive film on surface of the zircaloy-4 is an oxidation process. According to Pourbaix [10], there is an oxidation reaction that can

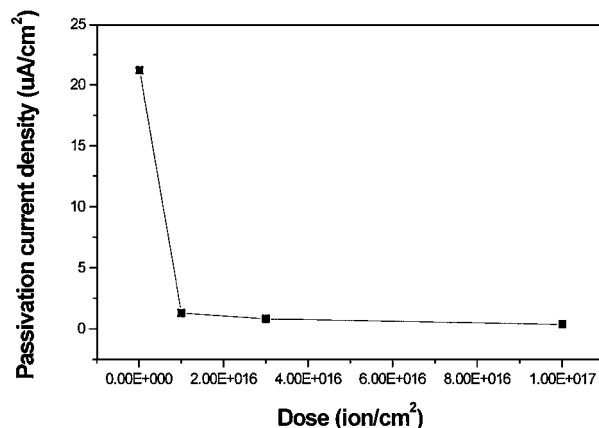
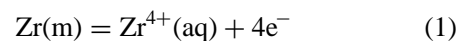
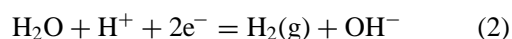


Figure 6 The dependence of the passivation current density,  $i_p$ , on the implanted doses.

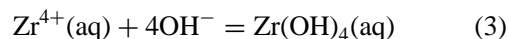
take place at the zirconium anode:



The cathodic reactions may be:



when the anode supplies sufficient  $\text{Zr}^{4+}$  cations to the solution,  $\text{Zr}(\text{OH})_4$  immediately becomes saturated in solution as follows [11]:



According to above facts, the growth of the film is partially determined by the migration of zirconium ions.

It has been reported that the reactive elements, such as yttrium, cerium and other rare earths, play an important role in the improvement of the corrosion properties [12, 13]. They are always applied as a coating, or present as an alloy or oxide dispersoid addition. In our case, the implanted yttrium applies as oxide dispersoid addition. As analyzed above, after yttrium ion implantation, the implanted yttrium exists in the form of  $\text{Y}_2\text{O}_3$  in the surface layer. The oxide dispersoid addition,  $\text{Y}_2\text{O}_3$ , acts as a barrier to reduce the migration and dissolution of zirconium. So, the passive current density decreases. When the implantation dose increases, the density of the oxide dispersoid,  $\text{Y}_2\text{O}_3$ , in the surface layer will increase, and the migration and dissolution of zirconium will be more difficult, as a result, the passive current density,  $i_p$ , reduces. In summary, the greater the concentration implanted yttrium ions, the smaller the passive current density (at the dose range from 0 to  $1 \times 10^{17}$  ions/cm<sup>2</sup>).

## 4. Conclusions

1. A significant improvement was achieved in the aqueous corrosion resistance of zircaloy-4 by yttrium ion implantation compared with that of the as-received zircaloy-4.

2. The implanted yttrium ions exist in the form of  $\text{Y}_2\text{O}_3$  in the surface layer.

3. The mechanism of the improvement of aqueous corrosion resistance probably attributable to the

addition of yttrium oxide dispersoid, but not to the structural transformation from polycrystalline to amorphous.

### Acknowledgements

The authors wish to thank Prof. X. J. Zhang for the kindness help in the implantation of yttrium ions. Financed by Institute of Low Energy Nuclear Physics, Radiation Beam and Materials Laboratory, Beijing Normal University.

### References

1. E. McCAFFERTY, P. M. NATISHAN and G. K. HUBLER, *Nuclear Instruments and Methods in Physics Research B* **56/57** (1991) 639.
2. Y. ETOH, S. SHIMADA and K. KIKUCHI, *Journal of Nuclear Science and Technology* **29**(12) (1992) 1173.
3. V. SSHWORTH, D. BAXTER, W. A. GRANT, R. P. M. PROCTER and T. C. WELLINGTON, *Corrosion Science* **16** (1976) 775.
4. G. K. HUBLER and E. McCAFFERTY, *ibid.* **20** (1980) 103.
5. X. D. BAI, D. H. ZHU and B. X. LIU, *Nuclear Instruments and Methods in Physics Research B* **103** (1995) 440.
6. Y. SUGIZAKI, T. YASUNAGA and H. TOMARI, *Surface and Coatings Technology* **83** (1996) 167.
7. M. F. STROOSNIJDER, J. D. SUNDERKOTTER, M. J. CRISTOBAL, H. JENETT, K. ISENBUGEL and M. A. BAKER, *ibid.* **83** (1996) 205.
8. M. J. CRISTOBAL, P. N. GIBSON and M. F. STROOSNIJDER, *Corrosion Science* **38** (1996) 805.
9. W. TIAN, W. P. CAI, J. LI and R. WU, *Materials Science and Engineering, A* **116** (1989) 5.
10. M. POURBAIX, "Atlas of Electrochemical Equilibria in Aqueous Solutions" (N.A.C.E., Houston, TX, 1974) p. 223.
11. C. F. BAES JR. and R. E. MESMER, "The Hydrolysis of Cations" (Wiley, New York, 1976) p. 147.
12. M. J. BENETT and A. T. TUSON, *Mater. Sci. Eng. A* **116** (1989) 79.
13. K. PRZYBYLSKI, A. J. FARRATT-REED and F. J. YUREK, *J. Electrochem. Soc.* **135** (1988) 509.

Received 10 March 1999  
and accepted 11 May 2000